



HAL
open science

Investigation of expression and activity levels of primary rat hepatocyte detoxication genes under various flow rates and cell densities in microfluidic biochips

Régis Baudoin, Giulia Alberto, Audrey Legendre, Patrick Paullier, Marie Naudot, Marie-José Fleury, Sébastien Jacques, Laurent Griscom, Eric Leclerc

► To cite this version:

Régis Baudoin, Giulia Alberto, Audrey Legendre, Patrick Paullier, Marie Naudot, et al.. Investigation of expression and activity levels of primary rat hepatocyte detoxication genes under various flow rates and cell densities in microfluidic biochips. *Biotechnology Progress*, 2013, 30 (2), pp.401-410. 10.1002/btpr.1857 . hal-03820745

HAL Id: hal-03820745

<https://hal.science/hal-03820745>

Submitted on 1 Aug 2023

HAL is a multi-disciplinary open access archive for the deposit and dissemination of scientific research documents, whether they are published or not. The documents may come from teaching and research institutions in France or abroad, or from public or private research centers.

L'archive ouverte pluridisciplinaire **HAL**, est destinée au dépôt et à la diffusion de documents scientifiques de niveau recherche, publiés ou non, émanant des établissements d'enseignement et de recherche français ou étrangers, des laboratoires publics ou privés.

Investigation of the levels of expression and activity of detoxication genes of primary rat hepatocytes under various flow rates and cell densities in microfluidic biochips

Regis Baudoin¹, Giulia Alberto¹, Audrey Legendre^{1*}, Patrick Paullier¹, Marie Naudot¹, Marie-José Fleury¹, Sébastien Jacques², Laurent Griscom³ and Eric Leclerc^{1*}

¹ CNRS UMR 7338, Laboratoire de Biomécanique et Bioingénierie, Université de Technologie de Compiègne, France

² INSERM U1016 Plate-forme génomique Institut Cochin, 22 rue Méchain, 75014 Paris, France

³ CNRS-UMR 8089, SATIE/BIOMIS, Ecole Normale Supérieure de Cachan-Bretagne, Campus de Ker Lann, Bruz, France

*Correspondence should be addressed to

Audrey Legendre or Eric Leclerc

CNRS UMR 7338, Laboratoire de Biomécanique et Bioingénierie, Université de Technologie de Compiègne, France

Email: audrey.legendre@utc.fr or eric.leclerc@utc.fr

Phone: 33 (0)3 44 23 79 43

Abstract

We have characterized the behavior of primary rat hepatocytes in biochips using a microfluidic platform (which we call IDCCM for integrated dynamic cell culture microchip). We investigated the effects of cell inoculation densities (0.2 to 0.5×10^6 cells/biochip), perfusion flow rates (10 , 25 and $40 \mu\text{L}/\text{min}$) during 72h of perfusion. No effect was observed on the hepatocytes morphologies, but the levels of mRNA and *CYP1A2* activity were found to be dependent of the initial cell densities and flow rates. Glucose consumption was independent of these parameters but albumin secretion was increased with the flow rate only from the first 24h of perfusion. The data set allows extracting a best estimated range of parameters in which the rat hepatocytes appeared the most functional in the biochips. Namely, at 0.25×10^6 inoculated cells cultivated under $25 \mu\text{L}/\text{min}$ during 72h , we demonstrated a better induction of the expression of all analyzed genes in comparison with others cell density and flow rate. Precisely, when primary rat hepatocytes were cultivated at these unoptimal condition, an important reduction of the mRNA levels was found for the xenosensors CAR and FXR, and their CYP-related (*CYP2E1*, *CYP7A1*, *CYP3A2* and *CYP2D2*). At $25 \mu\text{L}/\text{min}$ and 0.25×10^6 cells/biochip, the time lapse analysis demonstrated an over expression of *CYP3A1*, *CYP2B1*, *ABCC1b* and *ABCC2* in the biochips when compared to the post extraction levels. Furthermore the *AHR*, *CYP1A2*, *GSTA2*, *SULT1A1*, *UGT1A6* levels remained above 50% of the post extraction values whereas values of *HNF4a*, *CEBP* and *PXR* remained above 20% during all the culture duration. This study highlighted the functionality of primary rat hepatocytes in parallelized microfluidic culture conditions and confirmed the larger potential for cell application (primary human/rat hepatocytes, HepG2/C3a cell lines from our previous studies) with the IDCCM tools. Finally, these result illustrated the importance of this type of studies to establish parameters of microfluidic cultures before to perform/consider toxicological tests.

Keywords: Primary rat hepatocytes; IDCCM; microfluidic biochips; flow rates effect; density effect; gene expressions

1 Introduction

Safe use of new molecules developed by chemical, pharmaceutical, cosmetic and agronomic companies remain dependent on the screening and testing of these candidate compounds in model systems that are accurately predictive of how these agents will behave act in humans. To date, a classical step of this process has been achieved through animal testing. On June 2007, the European Community established new regulations on chemicals and their safe use called REACH (Registration, Evaluation, Authorization and Restriction of CHEMical substances). The REACH Regulation imposes a necessary high pressure on industry to manage the risks from chemicals and to provide safety information on the substances. To prevent an increased use of laboratory animals, the REACH commission urged industrials and scientists for a rapid development of alternatives to animal testing.

As a result, there is now a widespread need to develop methods that are not based on using animals and *in vivo* testing¹. To meet these needs, new *in vitro* tissue models have been developed at the interface between biomaterial engineering and medical science with a priority research direction related to the development of alternative *in vitro* approaches². The new *in vitro* models are designed to mimic specific organs or tissue responses to active principles or finished products and to ethically evaluate their innocuousness. These tools are the result of an intensive research effort initiated some decades ago at the interface between biomaterial engineering, tissue engineering and medical science.

Among those culture systems, hepatic microfluidic biochips have been proposed to reproduce several physiological characteristic and interactions such as liver zonation^{3,4}, 3D micro environment of hepatocytes and non parenchymal cells co-cultures^{5,6}, and functional bile duct network reconstruction⁷. The potential applications of hepatic biochips have been illustrated through xenobiotic screening *via* the determination of *in vitro* drug clearance^{8,9}, *via* cytotoxicity assays^{10,11}, or predictive toxicity assessments¹²⁻¹³.

Several parameters can be adjusted in those microfluidic biochips, including physical parameters such as the fabrication material, the design and the microchannel topography. In our previous works, we have developed a polydimethylsiloxane (PDMS) microfluidic biochip. We have shown theoretically that the oxygen diffusion in a PDMS biochip appeared sufficient to maintain suitable renal and hepatic oxygenation^{14,15}. Recently this analysis was confirmed in HepG3/C3a liver cell lines by coupling an intracellular metabolic flux analysis with data obtained from a metabolomics and transcriptomics profiling that demonstrated a higher cell oxygenation in the PDMS biochip when compared to conventional Petri dish culture methods¹⁶. A second group of parameters related to biological culture in biochips can be optimized, such as the initial cell densities or culture medium flow rates. Thus, the effect of cell density

was evidenced on drug metabolic processes^{17, 18} or on the state of hepatic differentiation¹⁹ in conventional Petri culture. The effect of flow rate is largely reported in hepatic bioreactors illustrating the importance of this parameter in maintaining hepatic differentiation (viability, oxygenation)²⁰ or to reproduce liver zonation³. In addition, we have demonstrated that HepG2/C3a biotransformation performance (*via* CYP1A assays) were flow rate and inoculation cell density dependent when cultivated in biochips²¹.

To increase our knowledge of hepatic tissues cultivated in microfluidic biochips, we have developed a platform based on the combination of polydimethylsiloxane (PDMS) microfluidic biochips and a polycarbonate packaging allowing parallelization²¹. In order to propose an optimized culture conditions using microfluidic biochips cultures, we propose to extend our parametrical study by using rat primary hepatocytes. Indeed, primary hepatocytes have a strong interest due to their structural and functional resemblance to *in vivo* liver²². In addition, primary cultures have been proven to be a powerful tool for analysis and characterization of the metabolic profile of drugs and chemicals with good *in vitro in vivo* extrapolation²³⁻²⁵. In this paper, we will characterize the viability, the levels of mRNA expression and hepatic differentiation, the CYP1A2 activity of rat primary hepatocytes under various inoculated cell densities and flow rates conditions.

2 Material and methods

2.1 Microfluidic biochips and IDCCM box

The biochips, the detailed concept of cell culture platform (IDCCM), the designs and microfabrication were described in our previous works^{21, 26}. Briefly, the biochips and the microfluidic structures are made in polydimethylsiloxane (PDMS) conventional moulding. The PDMS biochips were connected at the bottom of the IDCCM box by a simple series of “pluggable” ports. This format allowed an “easy plug and display” of the biochips. IDCCM is a manufactured polycarbonate box using a conventional 24-well plate format. Each microfluidic biochip was connected between two wells. Each of the 24 wells was used either as an entrance or an outlet reservoir allowing the parallelized culture of 12 independent biochips (Figs 1A, 1B). A specific cover was designed in order to allow the hermetic closure of the polycarbonate box for continuous flow perfusion. The cover includes ports for fluid perfusion and sampling. The hermetic closure of the IDCCM box and the pressure in the IDCCM box avoid any leakage or drain of the medium reservoir (Fig 1B).

2.2 Primary rat hepatocytes culture in IDCCM

The experiments were performed during a period of 5 days (Fig. 1C) which included three different phases: the hepatocyte extraction (day-0, post extraction), the adhesion phase (day-1, 24h of adhesion, 24h post extraction) and 72h of perfusion phase (from day-2 to day-4). The sterilization of the biochips, of the IDCCM box and the perfusion circuit was done by autoclaving the whole set up. The biochips were then connected to the box under sterile condition.

2.2.1 Primary rat hepatocytes isolation

Primary hepatocytes from 5-week-old male Sprague-Dawley rats weighing about 250g were isolated by a modification of the two-step *in situ* collagenase perfusion according to the method of Seglen²⁷. Animals were provided by the Janvier Elevage Animal Center (Le Genest Saint Isle, France). They were housed at the University of Compiègne with a 12h light / dark cycle at 22°C with food and water *ad libitum*. All experiments were approved by the Animal Experimental Committee of the University of Compiègne. The animal was anesthetized by intra peritoneal injection of sodium pentobarbital (Centravet, Gondreville, France). Briefly, after *in situ* washing and perfusion with collagenase solution at 30ml/min, the liver was extracted and the digested liver tissues were filtered through cotton gauze, then 400 and 100µm filters. The cell suspension was centrifuged and washed three times. Percoll isogradient centrifugation was performed to isolate dead cells and a significant portion of the non-parenchymal cells in a floating top layer was discarded. The resulting cells were finally suspended in the seeding medium as described below. Cell viability was assessed by trypan blue dye exclusion and hepatocytes with a viability of greater than 90% were used.

2.2.2 Inoculation of primary rat hepatocytes

Freshly isolated hepatocytes were cultured in first 24 hours in a seeding medium composed of William's E GLutamax medium (Fisher Scientific, Illkirch, France) supplemented with bovine insulin (5µg/ml, Sigma-Aldrich, Saint-Quentin Fallavier, France) and bovine fetal serum (10%). To enhance cell adhesion, the inner surface of the biochips were coated with rat tail type 1 (0.3mg/ml, BD Biosciences) prepared in phosphate-buffered saline (PBS) for 1 hour at 37°C in a humidified atmosphere supplied with 5% CO₂. After washing with seeding medium, the cells were inoculated inside the biochips at three

different hepatocyte inoculation densities: 0.2; 0.25 and 0.5×10^6 cells per biochip (*i.e.* 0.1, 0.125 and 0.25×10^6 per cm^2). After 24 hours, cells were cultured in William's E Glutamax medium supplemented with 3mg/ml Bovin Serum Albumin (Sigma-Aldrich), 5ng/ml dexamethasone (Sigma-Aldrich), 6.25 $\mu\text{g}/\text{ml}$ insulin-transferrin-selenium solution (Becton Dickinson, Biosciences, Le Pont de Claix, France), 100units/ml penicillin and 100mg/ml streptomycin (Fisher Scientific, Illkirch, France). During cell adhesion and cell culture, primary hepatocytes were incubated at 37°C in a humidified atmosphere supplied with 5% CO_2 .

2.2.3 Dynamic culture in IDCCM

After the 24h adhesion period, the IDCCM is prepared for the perfusion phase. Medium reservoirs at the entrance and outlet were filled with a volume of 2mL of culture medium to ensure the correct medium supply during dynamic culture resulting in a total volume of 4mL for each biochip. Then, the polytetrafluoroethylene (PTFE) tubes were connected to the fluidic cover of the IDCCM box and to the peristaltic pump. PTFE tubes were used to prevent loss of chemical compounds through diffusion or adsorption to the tubing used in the fluidic circuit. The entire system (pump and IDCCM box with the biochips) was placed into the incubator (37°C, 5% CO_2) and the perfusion started with the investigated flow rate. In this study we worked with three flow rates of 10, 25 and of 40 $\mu\text{l}/\text{min}$ with the cell density (0.2×10^6 cells per biochip). Culture medium was sampled and stocked at -20°C for posterior assays after adhesion phase and 24h, 48h and 72h of perfusion. Cytochrome assays and cell counting were performed on biochips (see below). Cells were photographed using a Leica DMI 6000B microscope together with the Leica camera and LAS life software (Leica Microsystems). Each analysis was repeated at least two times in triplicate biochips. Data was plotted as mean \pm standard error of the mean (SEM).

2.3 Cellular assays

2.3.1 Cell counting and viability

Cell counting was performed on a Malassez cell after cell detachment with trypsin-EDTA (Fisher Scientific). Cell viability was quantitatively analysed by trypan blue staining.

2.3.2 RTqPCR analysis

Total RNA was extracted using the Nucleospin® RNA XS isolation kit (Macherey-Nagel EURL, Hoerd, France). The quantity of RNA was assessed with a Nanodrop ND-1000 spectrophotometer (Nyxor Biotech, Paris, France). The quality of the RNA extracted was evaluated using the Agilent 2100 Bioanalyzer (using the Agilent RNA 6000 Nano and Pico kits). All RNA samples had an RNA Integrity Number of more than 8 (between 9.3 and 10).

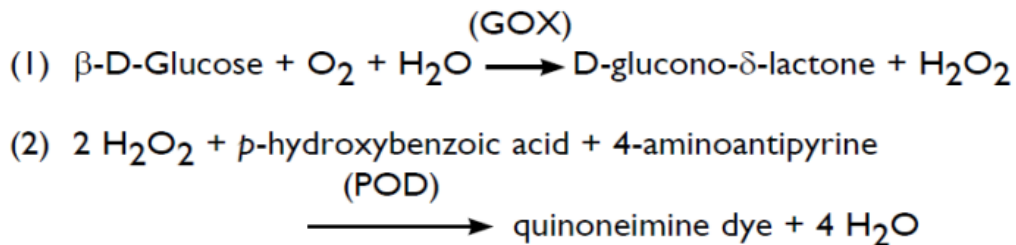
The cDNA samples were synthesized from 500ng of total RNA with oligodT Primer, using SuperScript II (Life Technologies), according to the manufacturer's protocol. Quantitative RT-PCR was performed using the LightCycler 480 Sybr Green I Master and the LightCycler 480 Probes Master (Roche), for the housekeeping genes and the targets genes respectively, and the Real Time PCR system LC480 (Roche). Pairs of primers for each of the 23 targets genes were designed using the Roche RealTime ready (UPL probes) Configurator tool (table 1) Couples of primers for housekeeping genes (*GAPDH*, *HPRT1*, *PPIB* and *SDHA*) were designed with Primer3, and tested for efficiency and specificity. The expression stability of these reference genes was assayed using GeNorm software application, which allows selecting the two most stable housekeeping genes in our model. All the couples were used in duplicate. Data from target genes were normalized with the two reference genes (*GAPDH* and *PPIB*). Data were analyzed using the ΔCt method²⁸ after validation of each duplicate (i.e. elimination of outliers' measures from duplicate with standard deviation above 0.4).

2.3.3 Cytochrome 1A2 assay

We add functional information to the RTqPCR data, we measured the basal levels of metabolic enzymatic activities. CYP1A2 activity was determined using 5-ethoxyresorufin (10 μM) as substrate. Resorufin formation by 7-ethoxyresorufin O-deethylation (EROD) was quantified with a fluorescence micro-plate reader (TECAN, Spectrafluor plus) after 1 hour's incubation at 37°C, CO₂ 5% in the presence of salicylamide (3mM) in order to inhibit phase II enzymes. All products were purchased from Sigma-Aldrich.

2.3.4 Glucose assay

In order to assess cell activity, glucose consumption was analyzed using a biochemical analyzer, the Konelab 20 (Thermo Fisher Electron Corporation, Courtaboeuf, France). Two different steps were involved in the reaction: the transformation of glucose in H_2O_2 and D-gluconate by the glucose oxidase (GOX), and then the transformation of H_2O_2 in quinone imine by the peroxidase (POD) as follow:



The absorbance of quinone imine is measured at a wavelength of 510nm. Each sample of culture medium was assessed in duplicate

2.3.5 Albumin assay

Albumin synthesis was assessed as specific hepatic marker. Albumin was measured using an ELISA sandwich test in a 96-well plate according to the rat albumin ELISA Quantitation Set protocol (Bethyl Laboratories, Euromedex, Souffelweyersheim, France). Briefly, albumin concentration of medium samples was analyzed in triplicate, utilizing a polyclonal antibody to rat albumin (ref. number: A110-134A and A110-134P). The absorbance was measured on a microplate reader (Tecan, Spectrafluor plus). Standard curves were generated using purified rat albumin diluted in culture medium. For each assay, the curve was generated as a 4-parameter curve fit using MasterPlex ReaderFit (Hitachi Solutions America, Ltd, MiraiBio Group (2012). Available from www.readerfit.com).

3. Results

Morphologies and rat hepatocytes cell number versus flow rates and inoculation cell densities.

The adhesion of the hepatocytes on the surface of the microfluidic biochips was successful for all inoculated densities. The Fig. 2 presents the cell morphology after three different inoculated densities. The cells uniformly occupied the surface of the biochip (as shown in Figs 2A, 2D and 2G). The hepatocytes shape was refringent between their cell junctions, with a typical cuboid shape and some binucleated hepatocytes were observed (Figs. 2C, 2F and 2I). The post adhesion cell count showed that only 40% of the cells were able to attach to the biochips surface when 0.5×10^6 cells were inoculated. However, an adhesion close to 80% was reached for 0.2 and 0.25×10^6 inoculated cells (Fig. 3A). At the end of the perfusion experiments, we observed a weak diminution of the cell number when 0.2×10^6 cells were inoculated whereas no difference between the post adhesion situations and after 72h of perfusion was detected when 0.25 and 0.5×10^6 cells were inoculated (Fig. 3A). In addition, when we investigated the cell response to 10; 25 and $40 \mu\text{L}/\text{min}$ flow rates, we did not observe any striking difference in the cell morphologies during the perfusion (Fig 4). Finally, we did not detect any effect of the flow rates on the final cell number as shown in Fig 3B.

Basal metabolism in rat hepatocytes in the IDCCM box and biochips

To validate rat hepatocyte functionality, we have investigated the basal metabolism by measuring the levels of glucose and albumin in the culture medium (Fig. 5). The glucose consumption was higher in the beginning of the culture with a reduction after 48h to 72h of perfusion. We did not detect striking effect of the flow rates (Fig 5A). The higher inoculated density contributed to increase the glucose consumption in the first 24h of perfusion whereas no effect of density was found after 72h of perfusion (Fig 5B). Concerning the albumin production we found that the highest flow rate increased the albumin production during the first 24h of perfusion. However, after 48h and 72h of culture any effect of flow rate was found (Fig. 5C). In addition, the time of cultured contribute to decrease the albumin production (Fig 5C). In addition, the increased of the inoculated density contributed to reduce the albumin production (Fig 5D).

To confirm the potential for drug metabolism in the biochips, we have measured the transformation of ethoxyresorufin into resorufin by *CYP1A2*. We found that biotransformation capabilities

were cell density dependent (Fig. 6). The normalized resorufin production measured post adhesion was reduced when the cell density increased. During the perfusion, this tendency was maintained at 25 μ L/min (Fig. 6A) and 10 μ L/min (data not shown). However, at similar cell density, a lower resorufin production was found at 10 and 40 μ L/min when compared to values measured at 25 μ L/min (Fig. 6B). In addition, the flow perfusion at 10 and 25 μ L/min contributed to maintain the level of resorufin production during the time of culture whereas 40 μ L/min led to a reduction of the resorufin production during the perfusion cultures (Fig. 6B). Finally, the resorufin production rate appeared larger in biochip when compared to Petri dish cultures after the adhesion step. This higher production was maintained in biochips for all tested flow rates as shown in Fig. 6C.

Dependency of rat hepatocytes mRNA levels are on flow rates, cell densities and culture time.

The RTqPCR was performed in order to investigate the levels of mRNA expression in the various investigated conditions. The mRNA levels were normalized by the post extraction levels.

The RTqPCR analysis performed after the hepatocyte adhesion step has shown that the variation of the cell density modified the initial mRNA profile (Fig. 7). It has been measured that the best situation corresponded to a cell inoculation density of 0.2 and 0.25 $\times 10^6$ cells/biochip whereas the lowest mRNA levels were obtained when 0.5 $\times 10^6$ cells were loaded. Then, the time lapse analysis demonstrated that after 48h of perfusion, the best inoculation condition remained the one corresponding to 0.25 $\times 10^6$ inoculated cells (Fig. 8). Indeed, the RTqPCR analysis performed on the hepatocytes inoculated at 0.2 $\times 10^6$ cells/biochip have shown mostly a lower range of the mRNA levels during the perfusion time when compared to the results obtained with 0.25 $\times 10^6$ inoculated cells. Particularly, at weak density (0.2 $\times 10^6$ cells/biochip), the expressions of xenosensors, CAR and FXR and their CYP-related to CAR and FXR (*CYP3A2*, *CYP7A1*, *CYP2C*, *CYP2E*) are downregulated. After 48 of perfusion, the variation of the perfusion conditions has shown that the increase of the flow rate contributed to increase the levels of the mRNA expression (xenosensors, CYP, ABC transporters, oxydative stress). In addition the increase of the flow rate reduce the down regulations observed for *CYP3A2*, *CYP7A1*, *CYP2C*, *CYP2E1* which are CYP-related to CAR and FXR expressions (Fig. 9). Thus, the 10 μ L/min flow rate contributed to lower expression levels whereas both 25 and 40 μ L/min flow rates appeared suitable to maintain high mRNA levels in our biochip configuration. Particularly, the level of hepatic transcription factor, *CEBP*, was downregulated at 10 μ L/min whereas was induced under 25 and 40 μ L/min. On contrary, the expressions of phase II enzymes, *SULT1A1* and *UGT1A6*, were decreased when the flow rate increase.

When we analyzed the mRNA expression levels at the best identified culture condition (0.25×10^6 cells/biochip and $25 \mu\text{L}/\text{min}$), the time lapse analysis showed that the levels of most of the investigated genes were reduced after the adhesion phases (Fig. 10). However, despite we found a down regulation, the percentage of the mRNA levels of transcription factors (*HNF4a* and *CEBP*) remained above 30% of post extraction levels. The nuclear receptors *AHR*, *PXR*, *CAR* remained above 80%, and the *CYP1A2*, *CYP2D1*, *SULT1A1* above 50%. In addition, the *CYP3A1/3A23*, *CYP2B1*, *UGT1A6*, *ABCCB1b*, *ABBC2*, *HMOX* and *NQO1* appeared up regulated after 24h of adhesion. On the contrary, a continuous decrease was measured for other genes. However, the levels remained above 20% for *HNF4a*, *CEBP* and *PXR* at the end of perfusion. Finally the most important reduction and the lowest mRNA levels were found for the *CYP2E1*, *CYP7A1*, *CYP3A2* and *CYP2D2*.

Discussion

The purpose of this study was to investigate hepatocyte behavior in the IDCCM culture conditions over 96h of culture including 24h of adhesion phase followed by 72h of perfusion. This experimental time was selected as most of the current *in vitro* analyses for acute toxicity are performed under short term culture and the xenobiotic exposures range between 24h to 96h²⁹⁻³¹. Thus, we have characterized the cell response to three main parameters that can be controlled easily in the IDCCM box and microfluidic biochips: the perfusion flow rates, the inoculated cell densities and the culture time in order to define best optimized culture conditions.

Comparatively with our data obtained with HepG2/C3a in the IDCCM box²², we didn't detect flow rate and cell density dependence of glucose consumption of primary rat hepatocytes in IDCCM. On contrary, albumin secretion seems more flow rate dependant when primary rat hepatocytes are cultivated in biochips, mainly strongly after 24h of perfusion. In addition, cell density of the primary hepatocytes inversely affected albumin secretion whereas this hepatic marker seemed cell density and cell proliferation dependent with HepG2/C3a cells²².

The global response of the rat hepatocytes in the biochips led to the best compromise in the culture conditions when the inoculated cell density ranged between 0.25 and 0.5×10^6 cells/biochip. Higher density led to a weak adhesion percentage resulting in a post adhesion cell number ranging between 160 000 to 200 000 rat hepatocytes in our biochips. This corresponded to 0.8 to 1×10^5 cells/cm². Particularly, after 48h of perfusion, we observed the down regulation of some genes at the cell

density of 0.2×10^6 cells/biochip (which was not detected at other cell densities). On the cell activity level, we demonstrated that at weak density, the glucose consumptions of primary rat hepatocytes is maximal after 48h of perfusion against 24h of perfusion for 0.5×10^6 cells/biochip. Glucose consumption measurement illustrated sufficient quantity of nutrients during the cultures. Oxygen shortage in the biochip can be a factor that limits the hepatocyte activity. Using the same model as our previous work¹⁵, we estimated a total amount of oxygen available via PDMS diffusion close to 3×10^{-5} mol/biochip/day which appeared to be in agreement with the 3.5×10^{-5} mol/biochip/day oxygen required for the cells located in the biochip (based on $0.4 \text{ nmol/s}/10^6$ cell oxygen consumption³, for the counted 2×10^5 cells).

The best flow rate to perform the culture out of the three flow rates was found to be $25 \mu\text{L}/\text{min}$. According to our previous simulations, at $25 \mu\text{L}/\text{min}$ in our biochip, we imposed a shear stress ranging between 30 to $50 \times 10^{-3} \text{ dyn}/\text{cm}^2$ (due to the complexity of the geometry). The RTqPCR analysis revealed higher level of expression of the mRNA of the investigated genes for $25 \mu\text{L}/\text{min}$ and $40 \mu\text{L}/\text{min}$ flow rate when compared to the $10 \mu\text{L}/\text{min}$ flow rate. However, the *CYP1A* functionality, assessed by resorufin production, clearly demonstrated a higher metabolism at $25 \mu\text{L}/\text{min}$ when compared to both 10 and $40 \mu\text{L}/\text{min}$ conditions. In addition, the *CYP1A* functionality appeared cell density dependent with a higher biotransformation capability at a lower cell density. As these results were obtained over 96h of culture, this study needs to be extended if longer times of perfusion are to be considered. Indeed we found that at too low cell density a reduction of the cell number in biochip occurred as the time elapsed. Thus the culture time must be taken into account in the choice of an optimized cell density and in function of the desired time point of the endpoint assays.

In spite of the fact that the expression of several mRNA was maintained at high levels when compared to post extraction situation (such as for *CYP3A1* or *CYP2B1*), we found during the time lapse analysis that the expressions of other mRNA continuously decreased after 72h of perfusion (such as the *CYP2C* and *CYP2D* families). Therefore, in the present culture configuration, this led to hypothesize that the best moment to perform drug and xenobiotic screening would be after 24h or 48h of perfusion when most of investigated genes remain above 40% of the post extraction values (such as *CYP3A1*, *CYP2B1*, *CYP1A2*, *SULT1A1*, *UGT1A6*, *GSTA2*, *ABC* transporters). In addition, this result was confirmed by the functional production of resorufin *via* the *CYP1A* activity. However, the entire set of results also illustrates the necessity to improve the quality of engineered hepatic tissue in the biochips in order to stabilize the cell differentiation and functionality for longer culture time. To do so, several research orientations can be explored. It may include the development of non-parenchymal cells co-culture³⁰, the optimization of the culture medium (by testing additives such as DMSO, HGF, glucagon, hormones

etc...³¹⁻³⁴) or the integration of a new design element in the IDCCM box and biochips based on literature improvement^{6, 7, 35}.

In order to identify the added value of the present biochip and culture format, we have to compare more deeply the hepatic functions reached in our biochips with various *in vitro* methods such as Petri, other microchips or bioreactors. Indeed, even if we reached in the biochips the post extraction levels of several mRNA levels, we need to establish the functional performance of the biochips. In this study, when compared Petri, we showed a systematic higher functionality of the CYP1A in the IDCCM microfluidic biochips. Such higher performance when compared to conventional Petri is now well established as far as several studies using microfluidic biochips also reported those types of results²¹. In addition, the positive effect of dynamic cultures on hepatic tissue in our biochips is consistent with other literature reports^{3, 36-38}. Nevertheless, direct comparisons are difficult as far as cell density, biochip geometries and materials, shear stress and fluid flow rates, or oxygenation supply, are always different in all of those studies. This non exhaustive literature analysis contributes to extract potential range suitable for hepatocytes microfluidic cultures. Thus, we found functional rat hepatocytes cultures in the literature in the shear stress range between 5.6×10^{-4} and 0.33 dyn/cm^2 , and using an inoculated cell density range between 0.025 and $0.2 \times 10^6 \text{ cells/cm}^2$, as well as an adequate oxygen supply (around probably $0.4 \text{ nmol/s}/10^6 \text{ cells}^3$) either by using integrated membranes, fluid oxygenator or permeable fabrication material (such as PDMS). Therefore, the key feature for optimization of the hepatic microfluidic cultures appeared to be able to maintain a balance between those parameters. Finally, the range of parameter that we extracted from our study is in agreement with the literature reports.

Conclusions

In this work we have investigated the response of rat primary hepatocytes to various culture conditions inside our microfluidic biochip platform. The integration of the morphologic analysis, the RTqPCR investigation and the CYP functional assays contributed to extract a range of working conditions in our biochip set up. When 250 000 cells were inoculated and cultivated at $25 \mu\text{L}/\text{min}$ we found a high level of the mRNA expression related to drug metabolism including the transcription factors (such as *HNF4a*, *PXR*), the phase I (such as *CYP P450*) and phase II (such as *UGT*) genes when compared to post extraction situation. The analysis of the functionality of CYP1A, controlled by resorufin production from 7-ethoxyresorufin O-deethylation, demonstrated higher biotransformation in biochips

when compared to conventional Petri dishes conditions. The data set of this study provides evidence of rat hepatocyte performance in the microfluidic biochips when compared to Petri methods and of post extraction hepatocytes.

Acknowledgments:

This work was supported by the « Fondation pour la Recherche et l'Innovation » de l'Université de Technologie de Compiègne, by the UTEAM-Carnot grant "Parachip". Régis Baudoin was funded by the CNRS via a research valorization program. Giulia Alberto was granted by the ERASMUS program between l'Université de Technologie de Compiègne and Polytechnico Torino

References:

1. Blaauboer BJ , The integration of data on physico-chemical properties, in vitro-derived toxicity data and physiologically based kinetic and dynamic as modelling a tool in hazard and risk assessment. A commentary. *Toxicology Letters* , 2003, **138**, 161-171.
2. Bhogal N, Grindon C, Combes R and Balls M , Toxicity testing: creating a revolution based on new technologies. *Trends in Biotechnology* , 2005, **23**, 299-307.
3. Allen JW, Khetani .SR, Bhatia SN, In Vitro Zonation and Toxicity in a Hepatocyte Bioreactor. *Toxicological Sciences*, 2005, **84**, 110-119.
4. Cheng S, Prot J-M, Leclerc E, Bois FY, Zonation related function and ubiquitination regulation in human hepatocellular carcinoma cells in dynamic vs. static culture conditions. *BMC Genomics*, 2012, **13**, 54-61.
5. Powers MJ, Janigian DM, Wack KE, Baker CS, Stolz DB, Griffith LG, Functional Behavior of Primary Rat Liver Cells in a Three-Dimensional Perfused Microarray Bioreactor. *Tissue Engineering*, 2002, **8**, 499-513.
6. Domansky K, Inman W, Serdy J, Dash A, Lim MH, Griffith LG, Perfused multiwell plate for 3D liver tissue engineering. *Lab on Chip.*, 2010, **10**, 51-58.
7. Nakao Y, Kimura H, Sakai Y, Fujii T., Bile canaliculi formation by aligning rat primary hepatocytes in a microfluidic device , *Biomicrofluidics*, 2011, **5**, 022212-9

8. Chao P, Maguire T, Novik E, Cheng KC, Yarmush ML, Evaluation of a microfluidic based cell culture platform with primary human hepatocytes for the prediction of hepatic clearance in human. *Biochemical Pharmacology*, 2009, **78**, 625-632.
9. Baudoin R, Prot JM, Nicolas G, Brocheton J, Brochot C, Legallais C, Benech H, Leclerc E, Evaluation of seven drug metabolisms and clearances by cryopreserved Human primary hepatocytes cultivated in microfluidic biochips. *Xenobiotica*, 2012a, in press.
10. Toh YC, Lim TC, Tai D, Xiao G, van Noort D, Yu H, A microfluidic 3D hepatocyte chip for drug toxicity testing. *Lab on Chip*, 2009, **9** 2026-2035.
11. Zhang SF, Tong WH, Zheng BX, Susanto TAK, Xia L, Zhang C, Ananthanarayanan A, Tuo XY, Sakban RB, Jia RR, Iliescu C, Chai KH, McMillian M, Shen SL, Leo H, Yu H. A robust high-throughput sandwich cell-based drug screening platform. *Biomaterials*, 2011, **32**, 1229-1241.
12. Prot JM, Bunescu A, Elena-Herrmann B, Aninat C, Choucha Snouber L, Griscom L, Razan F, Bois FY, Legallais C, Brochot C, Corlu A, Dumas ME, Leclerc E, Predictive toxicology using systemic biology and liver microfluidic "on chip" approaches: application to acetaminophen injury, *Toxicol Appl Pharmacol.*, 2012, **259**, 270-280.
13. Shintu L, Baudoin R. Navratil V, Prot JM, Pontoizeau C, Defernez M, Blaise BJ, Domange C, Pery AR, Toulhoat P, Legallais C, Brochot C, Leclerc E, Dumas ME, . Metabolomics-on-a-chip and predictive systems toxicology in microfluidic bioartificial organs. *Anal Chem*, 2012, **84**, 1840-1848.
14. Baudoin R, Griscom L, Monge M, Legallais C, Leclerc E, Development of a renal microchip for in vitro distal tubule models, *Biotechnology Progress*, 2007, **23**, 1245-1253
15. Leclerc E, Sakai Y, and Fujii T, Cell culture in 3-dimensional microfluidic structure of PDMS (polydimethylsiloxane), *Biomedical Microdevices*, 2003, **5**, 109-114
16. Ouattara D, Prot JM, Bunescu A, Dumas ME, Elena-Herrmann B, Leclerc E and Brochot C, Metabolomics-on-a-chip and metabolic flux analysis for a label-free modeling of the internal metabolism of HepG2/C3A cells in an in vitro microfluidic biochip, *Molecular Biosystems*, 2012, **8**, 1908-1920
17. Jurin RR, McCune SA, Effect of cell density on metabolism in isolated rat hepatocytes, *J Cell Physiol.* 1985 Jun;123,3:442-8
18. Greuet J, Pichard L, Ourlin JC, Bonfils C, Domergue J, Le Treut P, Maurel P., Effect of cell density and epidermal growth factor on the inducible expression of CYP3A and CYP1A genes in human hepatocytes in primary culture. *Hepatology.* 1997, **25**, 1166-75.

19. Nakamura T, Yoshimoto K., YASUO Nakayama Y., Tomita Y, Ichiara A, Reciprocal modulation of growth and differentiated functions of mature rat hepatocytes in primary culture by cell-cell contact and cell membranes, *Proc. Nati. Acad. Sci. USA* , 1983, **80**, 7229-7233
20. Tilles AW, Baskaran H, Roy P, Yarmush ML, Toner M, Effects of oxygenation and flow on the viability and function of rat hepatocytes cocultured in a microchannel flat-plate bioreactor. *Biotechnol Bioeng*, 2001, **73**, 379-389.
21. Baudoin R, Alberto G, Legallais C, Leclerc E, Parallelized microfluidic biochips in multi well plate applied to liver tissue engineering. *Sensors and Actuators B*, **173**, 919– 926, 2012
22. Brandon E, Raap C, Meijerman I, Beijnen J, Schellens J, An update on in vitro test methods in human hepatic drug biotransformation research: pros and cons. *Toxicology and Applied Pharmacology*, 2003, **18**, 233–246
23. Chenery RJ, Ayrton A, Oldham HG, Standring P, Norman SJ, Seddon T, Kirby R, Diazepam metabolism in cultured hepatocytes from rat, rabbit, dog, guinea pig, and man. *Drug Metab. Dispos.*, 1987, **15**, 312–317.
24. Bayliss, M.K., Bell, J.A., Jenner, W.N., Park, G.R., Wilson, K.,. Utility of hepatocytes to model species in the metabolism of loxidine and to predict pharmacokinetic parameters in rat, dog and man. *Xenobiotica* , 1999, **29**, 253–268.
25. Cross DM, Bell JA, Wilson K, Kinetics of ranitidine metabolism in dog and rat isolated hepatocytes. *Xenobiotica*, 1995, **25**, 367–375.
26. Baudoin R, Griscom L, Prot JM, Legallais C, Leclerc E, Behavior of HepG2/C3A cell cultures in a microfluidic bioreactor. *Biochem Eng. Journal*, 2011, **53**, 172-181
27. Seglen PO, Preparation of rat liver cells. 3. Enzymatic requirements for tissue dispersion. *Exp Cell Res*, 1973, **82**, 391-398.
28. Pfaffl MW, A new mathematical model for relative quantification in real-time RT-PCR. *Nucleic Acids Res*, 2001, **29**, e45.
29. Barile F, Dierickx P, Kristen U, In vitro cytotoxicity testing prediction of acute human toxicity, *Cell Biol and Toxicology*, 1994, **10**, 155-162
30. Clemedson C., et al, MEIC evaluation of acute systemic toxicity. Part III. ATLA, 1998, **26**,93–129.
31. Clemedson C., et al, MEIC evaluation of acute systemic toxicity. Part IV., 1998, ATLA **26**,131–183.
32. Bhandari R, Riccalton L, Lewis A, Fry J, Hammond A, Tendler S, Shakesheff K, Liver Tissue Engineering: A Role for Co-culture Systems in Modifying Hepatocyte Function and Viability, *Tissue Engineering*, 2001, **7**, 345-357

33. Dong J, Mandenius CF, Lübberstedt M, Urbaniak T, Nüssler A, Knobloch D, Gerlach J, Zeilinger K, Evaluation and optimization of hepatocyte culture media factors by design of experiments (DoE), *methodology*, 2008, **57**, 3, 251-261
34. Ahluwalia A, Clodfelter KH, Waxman DJ, Sexual dimorphism of rat liver gene expression: regulatory role of growth hormone revealed by DNA microarray analysis, *Molec Endocrinol*, 2004, **18**, 747-760
35. Lee P, Hung J, Lee L, An Artificial Liver Sinusoid With a Microfluidic Endothelial-Like Barrier for Primary Hepatocyte Culture, *Biotechnology and Bioengineering*, 2007, **97**, 1340-1346
36. Sivaraman A, Leach JK, Townsend S, Iida T, Hogan BJ, Stolz DB, Fry R, Samson LD, Tannenbaum SR, Griffith LG, A microscale in vitro physiological model of the liver: predictive screens for drug metabolism and enzyme induction. *Curr. Drug Metab*, 2005, **6**, 569-591.
37. Xia L, Ng S, Han R, Tuo X, Xiao G, Leo HL, Cheng T, Yu H, Laminar-flow immediate-overlay hepatocyte sandwich perfusion system for drug hepatotoxicity testing, *Biomaterials*, 2009, **30**, 5927-5936
38. Ahluwalia A, Daujat-Chavanieu M, Modular bioreactor for primary human hepatocyte culture: Medium flow stimulates expression and activity of detoxification genes, *Biotechnol J.*, 2011, **6**: 554–564

Figures and table list:

Table 1: List of 23 targeted genes studied using the RealTime ready probes from Roche.

Figure 1: (A) Schematic principle of the IDCCM box coupled with a microfluidic biochip; (B) IDCCM Box with biochips and pump used for cell cultures; (C) Experimental procedure

Figure 2: Hepatocyte morphologies after adhesion during 24h (A-C) of 200 000 inoculated cells; (D-F) of 250 000 inoculated cells and (G-I) of 500 000 inoculated cells (images taken before start the perfusion at three magnifications x10; x20; x40).

Figure 3: (A) Effect of inoculated density on cell number collected in biochip after adhesion and 72h of perfusion at 25µL/min; (B) Effect of flow rates on cell collected numbers for a 200 000 inoculated cells.

Figure 4: typical morphologies of rat hepatocytes in the biochips inoculated at 250 000 cells/biochip, perfused at 10, 25 and 40 µL/min after 48h and 72h of perfusion

Figure 5: Glucose consumption of rat hepatocytes (A) for three flow rates at 0.2×10^5 inoculated hepatocytes/biochip; (B) at 25µL/min for two inoculated cell density; Albumin production of rat hepatocytes (C) effect of flow rate at 0.2×10^5 cells/biochip; (D) effect of inoculated cell density at 25µL/min.

Figure 6: Levels of resorufin production by CYP1A2 of rat hepatocytes (A) at 25µL/min independently of the culture time; (B) for various flow rates with 0.2×10^6 inoculated cells (C) after 24h post adhesion in biochips when compared to Petri

Figure 7: Comparison of the levels of mRNA of rat hepatocytes in the biochips after adhesion for three inoculated densities. Data expressed the percentage of induction when compared to post extraction values

Figure 8: Comparison of the levels of mRNA of rat hepatocytes in the biochips during the time of cultures (inoculated density of 250 000 cells/biochip, flow rate at 25µL/min). Data expressed the percentage of induction when compared to post extraction values

Figure 9: Comparison of the levels of mRNA of rat hepatocytes in the biochips after 48h of perfusion under three flow rates (cells inoculated at 0.2×10^6 cells/biochip). Data expressed the percentage of induction when compared to post extraction values

Figure 10: Comparison of the levels of mRNA of rat hepatocytes in the biochips after 48h of perfusion at 25µL/min for three inoculated densities. Data expressed the percentage of induction when compared to post extraction values

Functions	Gene Symbol	Assay ID (RTR)	Amplicon Size (pb)	Accession ID
Hepatic Transcription factors	HNF4a	500286	92	ENSRNOT00000011978
	CEBP	503796	112	ENSRNOT00000030773
Xenosensors	AHR	503494	73	ENSRNOT00000006618
	PXR - NR1I2	503757	95	ENSRNOT00000003934
	CAR – NRI3	503790	95	ENSRNOT00000049873
	FXR - NR1H4	503760	92	ENSRNOT00000009910
CYPs	CYP1A2	503414	60	ENSRNOT00000058571
	CYP3A2	503762	82	ENSRNOT00000001291
	CYP3A23/3A1	502664	65	ENSRNOT00000051244
	CYP7A1	503785	78	ENSRNOT00000012819
	CYP2B1	503749	61	ENSRNOT00000047540
	CYP2C6	503746	96	XM_001066767
	CYP2C	502669	94	ENSRNOT00000017310
	CYP2D1	503742	83	ENSRNOT00000050002
	CYP2D2	503737	60	ENSRNOT00000012413
	CYP2E1	503000	61	ENSRNOT00000016883
Phase II Enzymes	GSTA2	502674	78	ENSRNOT00000044944
	SULT1A1	503770	76	ENSRNOT00000026186
	UGT1A6	503773	96	NM_001039691
ABC transporters	Pgp - ABCB1b	502651	69	ENSRNOT00000037712
	MRP2- ABCC2	503769	64	NM_012833
Oxidative stress - Inflammation	HMOX1	502648	71	ENSRNOT00000019192
Oxidative stress	NQO1	502688	77	ENSRNOT00000017174

Table 1: List of 23 targeted genes studied using the RealTime ready probes from Roche.

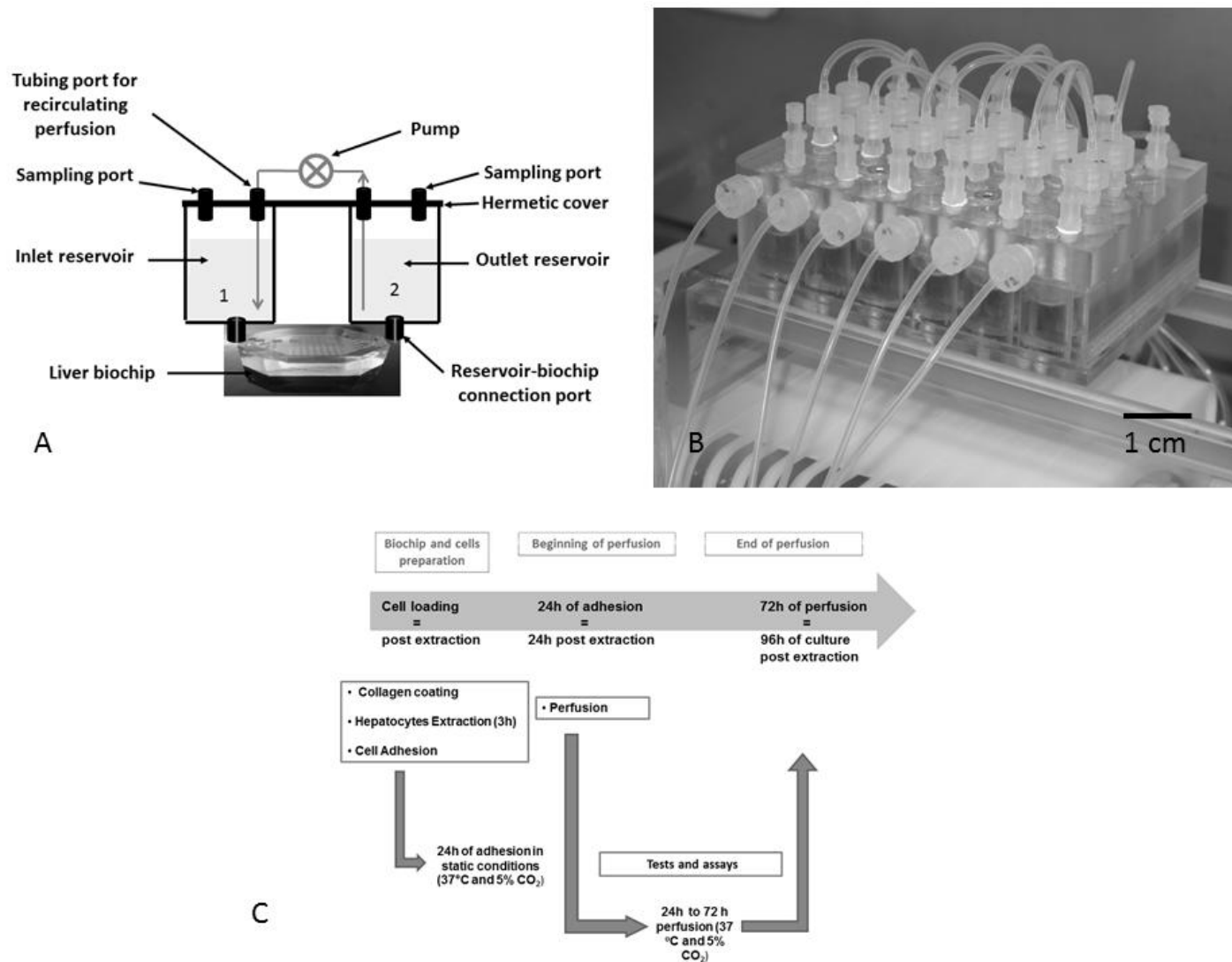


Figure 1: (A) Schematic principle of the IDCCM box coupled with a microfluidic biochip; (B) IDCCM Box with biochips and pump used for cell cultures; (C) Experimental procedure.

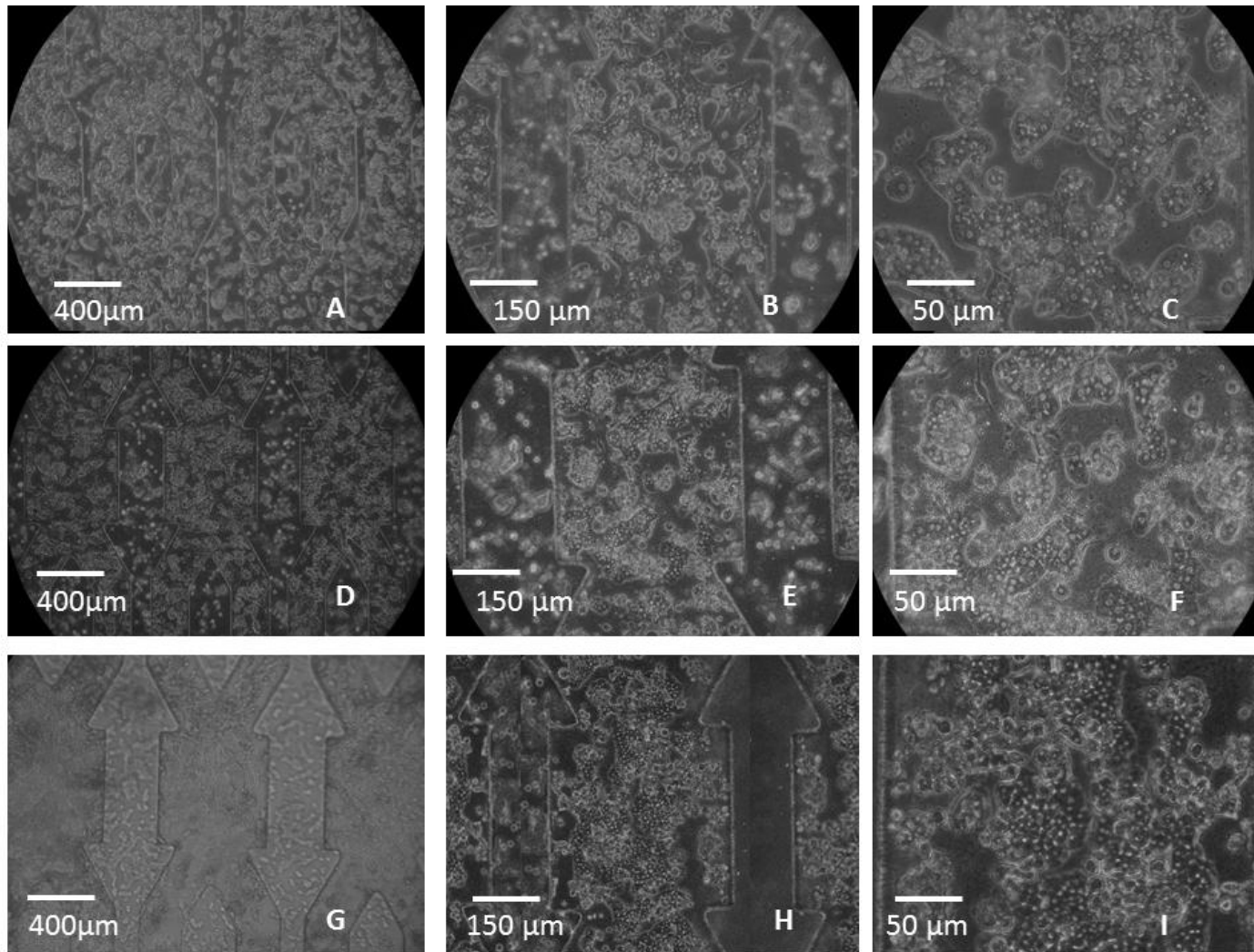
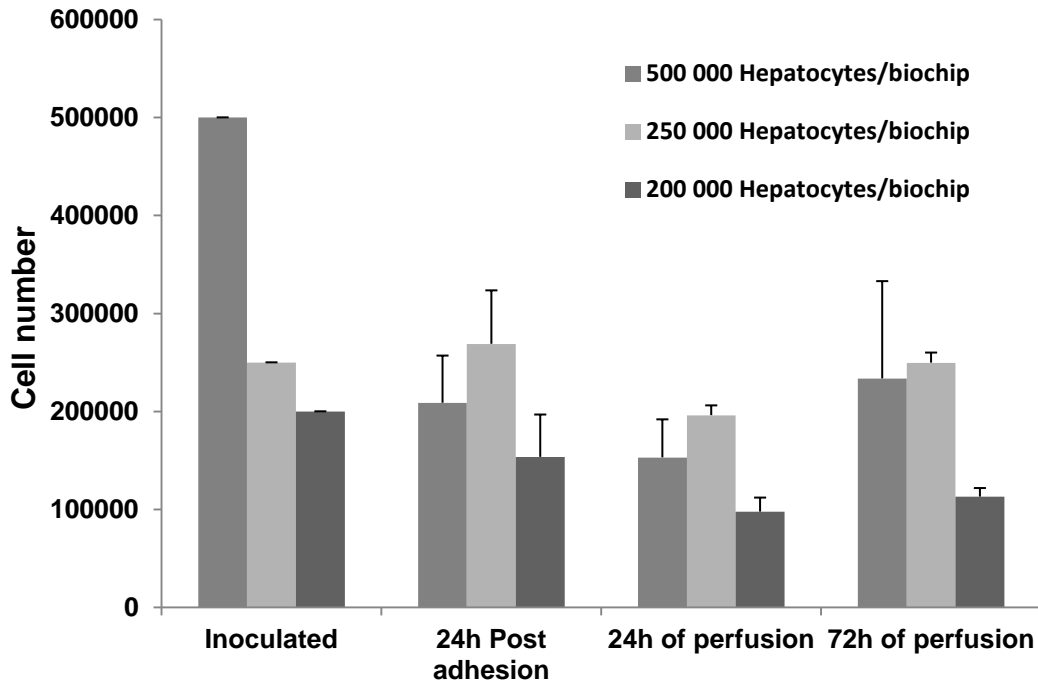


Figure 2: Hepatocyte morphologies after adhesion during 24h (A-C) of 200 000 inoculated cells; (D-F) of 250 000 inoculated cells and (G-I) of 500 000 inoculated cells (images taken before start the perfusion at three magnifications x10; x20; x40).

A



B

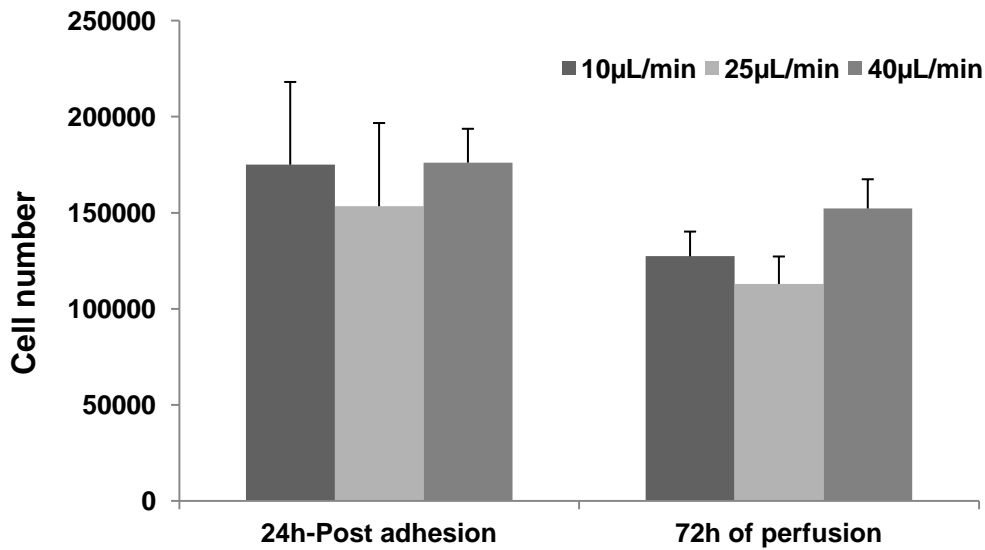


Figure 3: (A) Effect of inoculated density on cell number collected in biochip after adhesion and 72h of perfusion at 25 $\mu\text{L}/\text{min}$; (B) Effect of flow rates on cell collected numbers for a 200 000 inoculated cells.

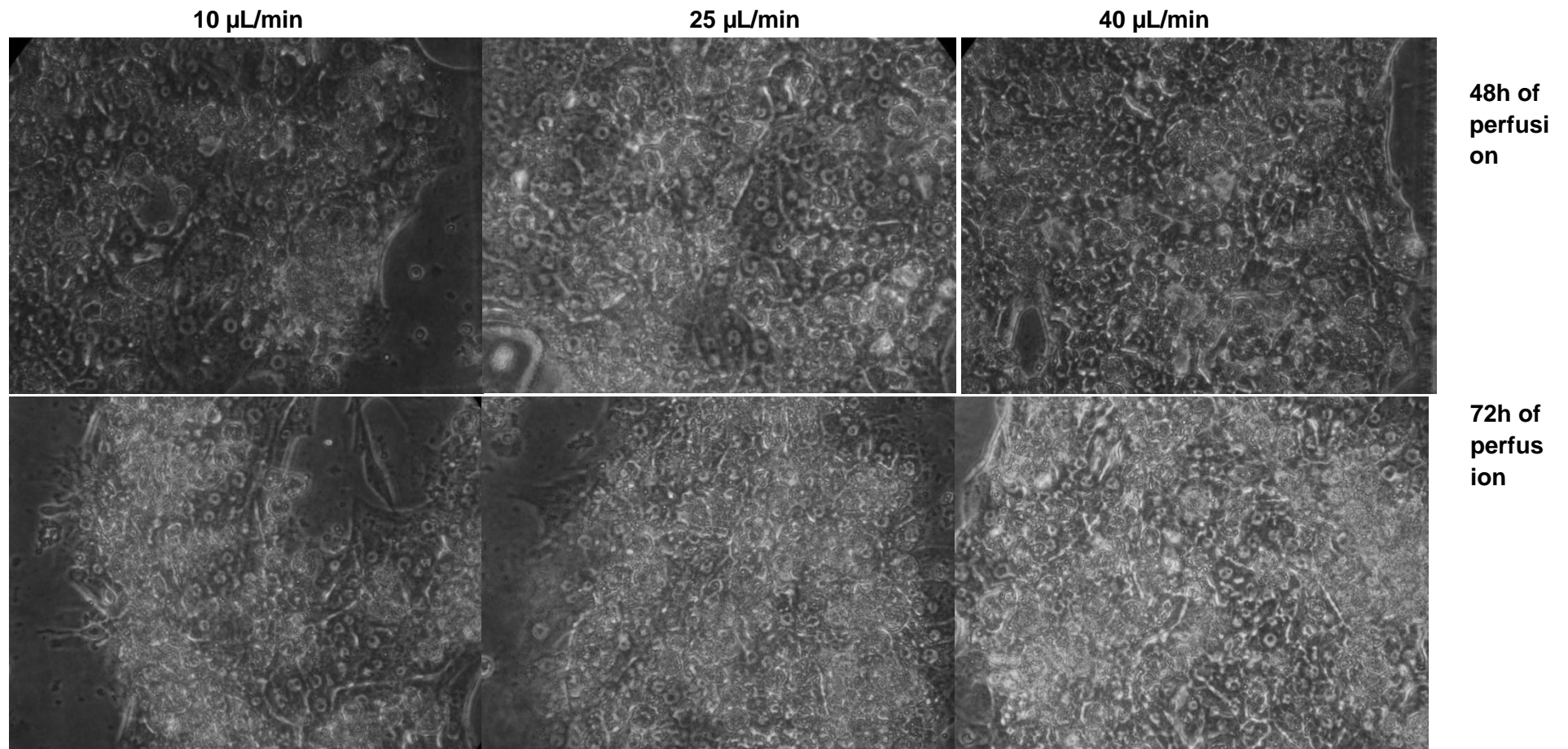


Figure 4: typical morphologies of rat hepatocytes in the biochips inoculated at 250 000 cells/biochip, perfused at 10, 25 and 40 $\mu\text{L}/\text{min}$ after 48h and 72h of perfusion

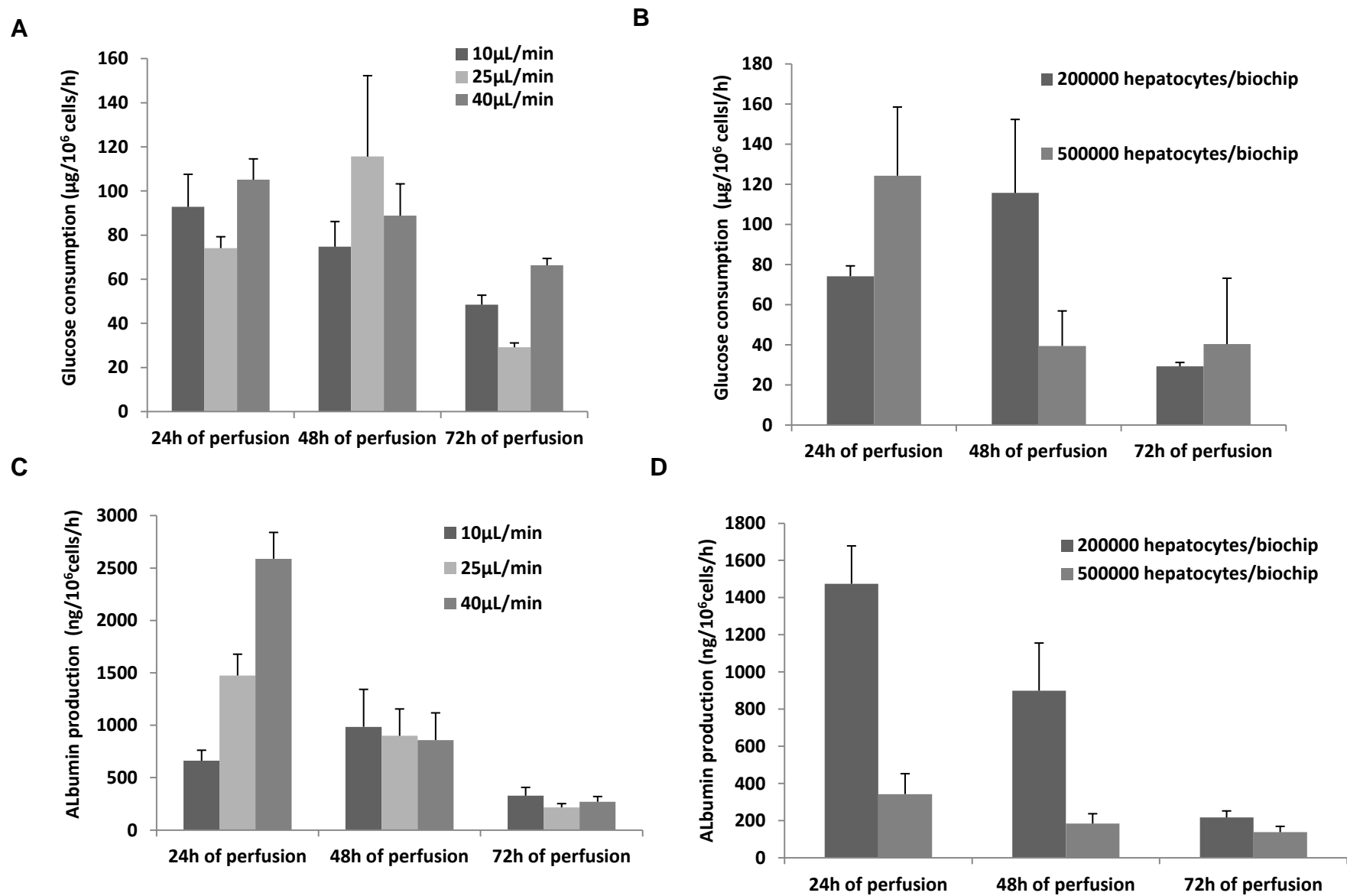


Figure 5: Glucose consumption of rat hepatocytes (A) for three flow rates at 0.2×10^6 inoculated hepatocytes/biochip; (B) at $25 \mu\text{L}/\text{min}$ for two inoculated cell density; Albumin production of rat hepatocytes (C) effect of flow rate at 0.2×10^6 cells/biochip; (D) effect of two inoculated cell density at $25 \mu\text{L}/\text{min}$.

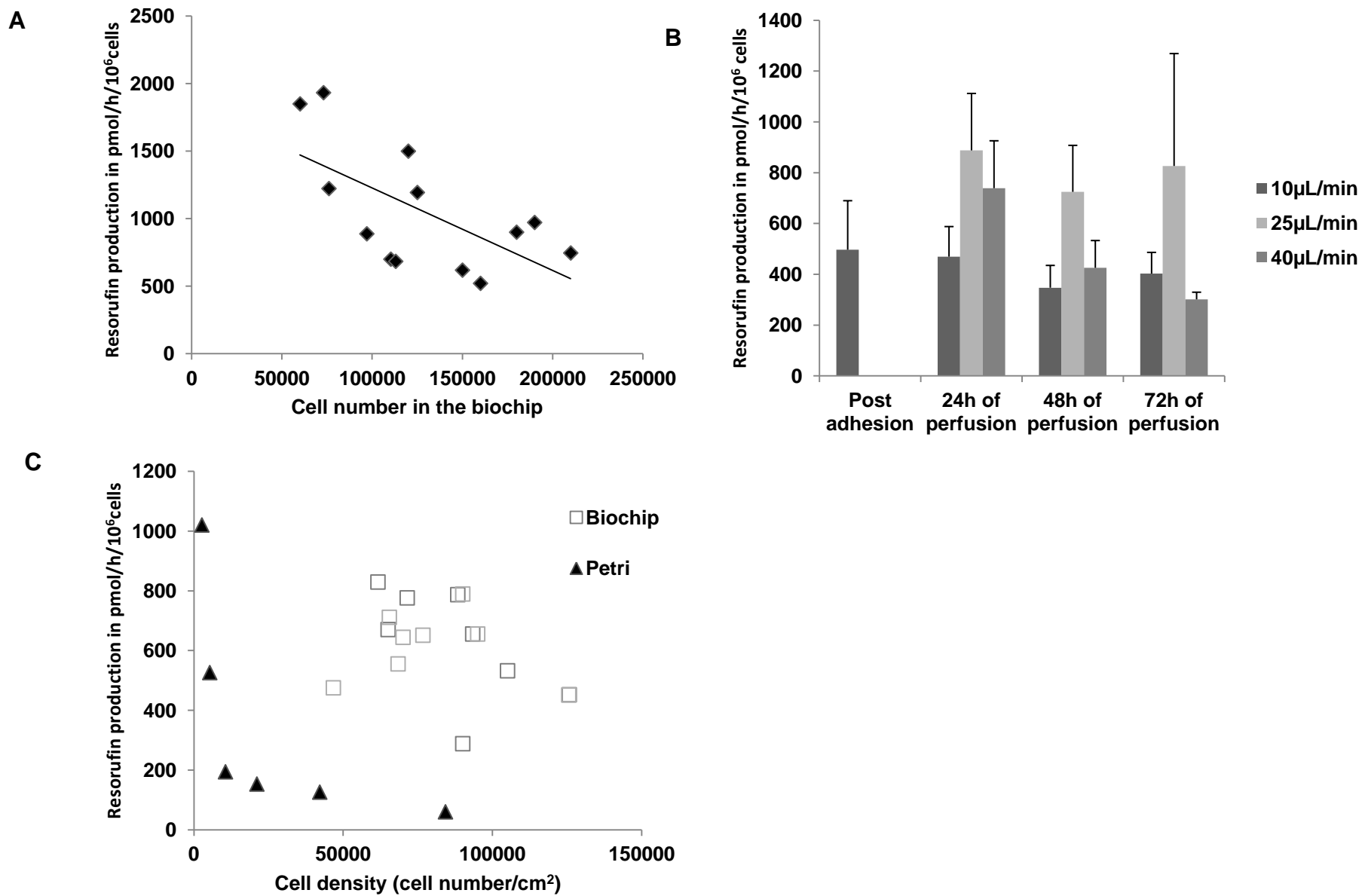


Figure 6: Levels of resorufin production by *CYP1A2* of rat hepatocytes (A) at 25μL/min independently of the culture time; (B) for various flow rates with 0.2x10⁶ inoculated cells (C) after 24h post adhesion in biochips when compared to Petri

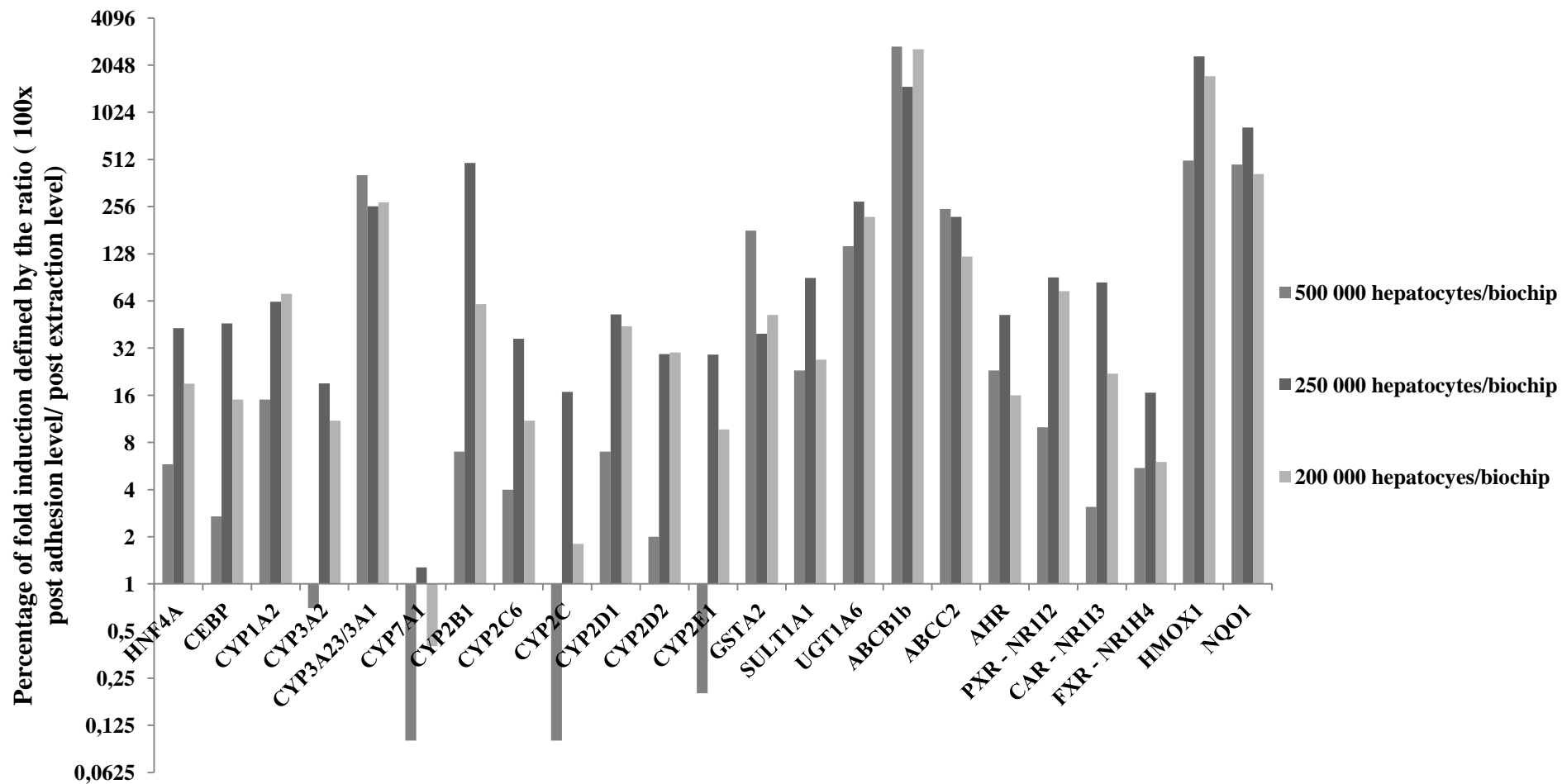


Figure 7: Comparison of the levels of mRNA of rat hepatocytes in the biochips after adhesion for three inoculated densities. Data expressed the percentage of induction when compared to post extraction values

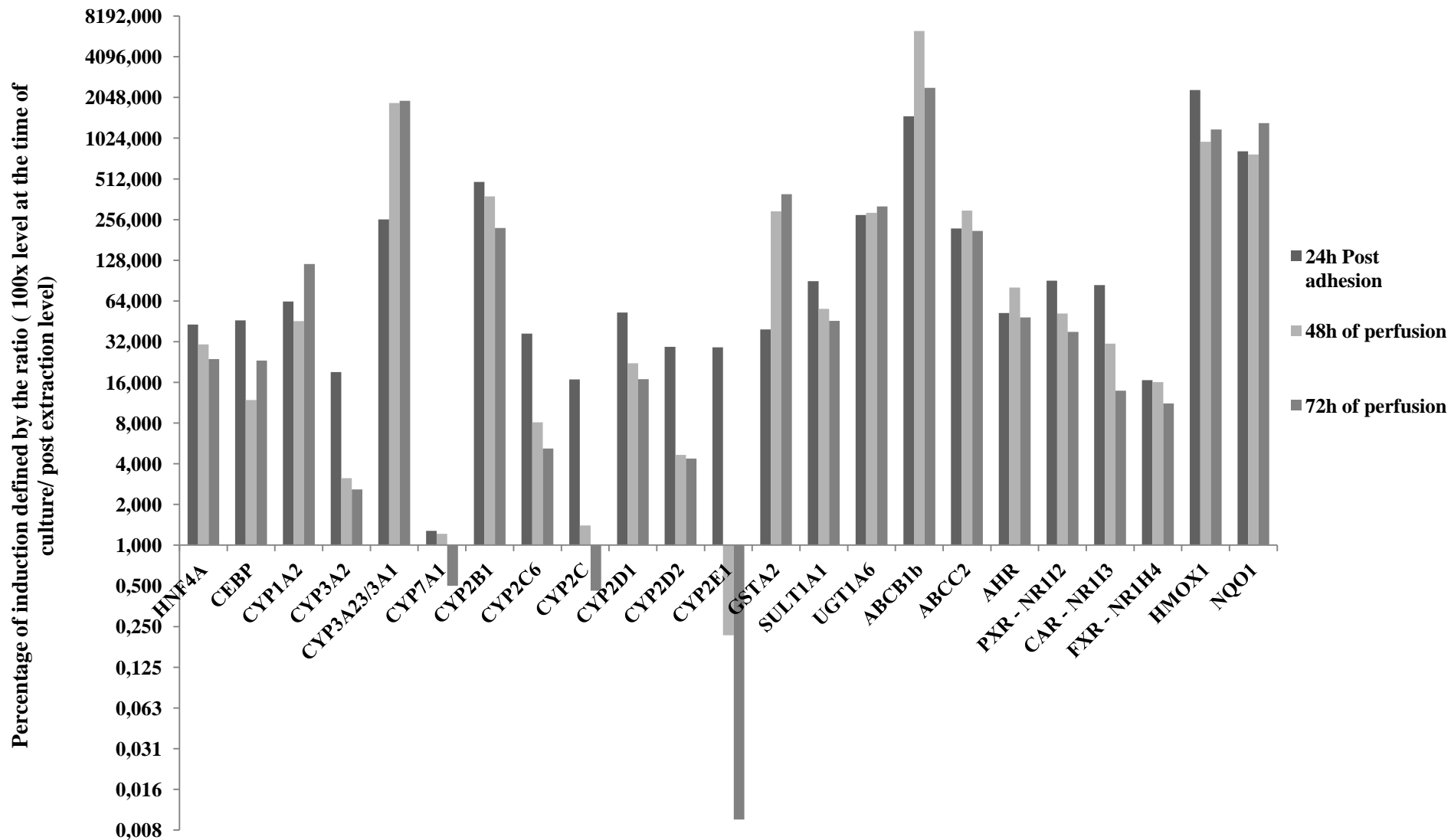


Figure 8: Comparison of the levels of mRNA of rat hepatocytes in the biochips during the time of cultures (inoculated density of 250 000 cells/biochip, flow rate at 25 μ L/min). Data expressed the percentage of induction when compared to post extraction values

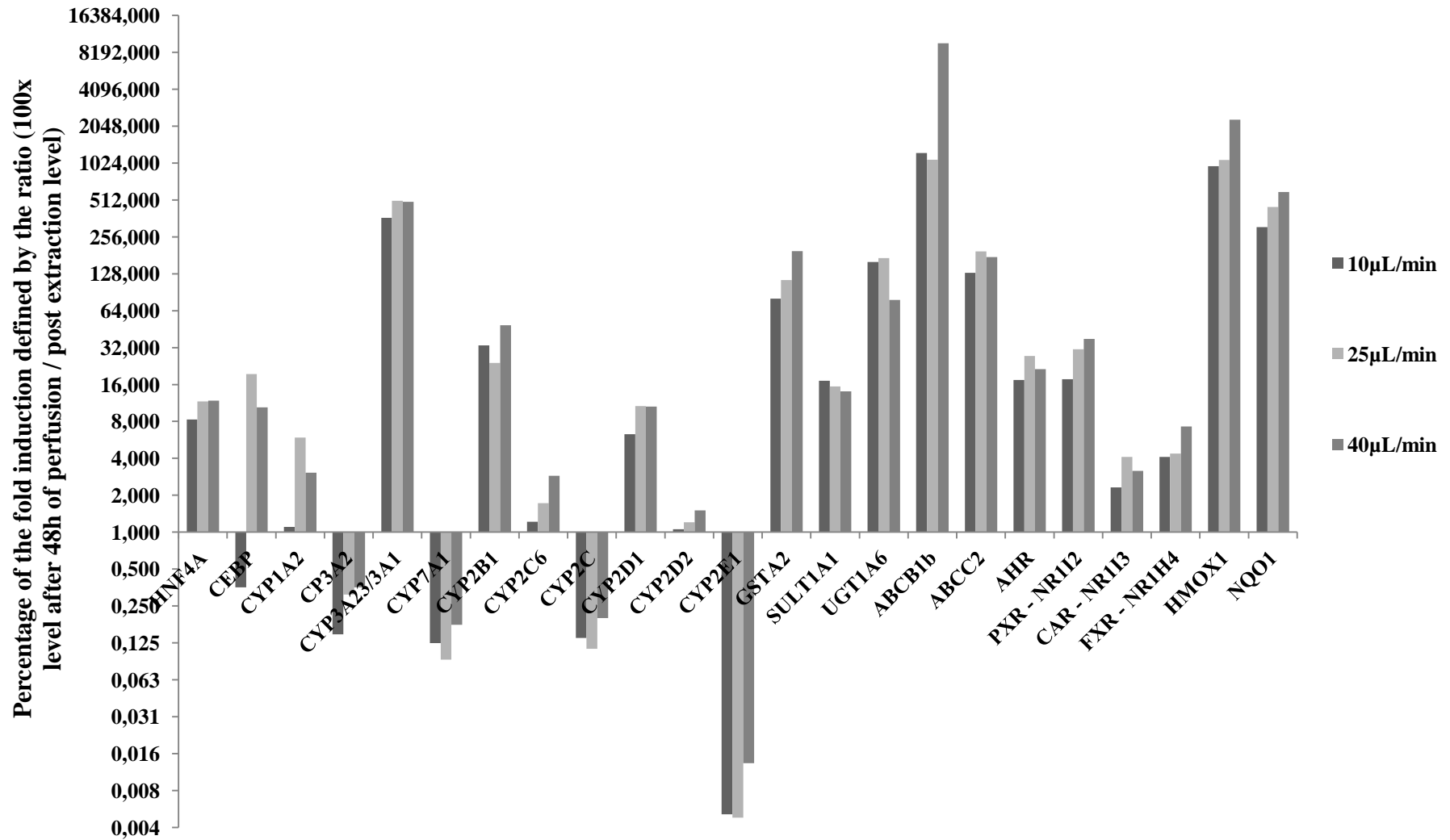


Figure 9: Comparison of the levels of mRNA of rat hepatocytes in the biochips after 48h of perfusion under three flow rates (cells inoculated at 0.2×10^6 cells/biochip). Data expressed the percentage of induction when compared to post extraction values

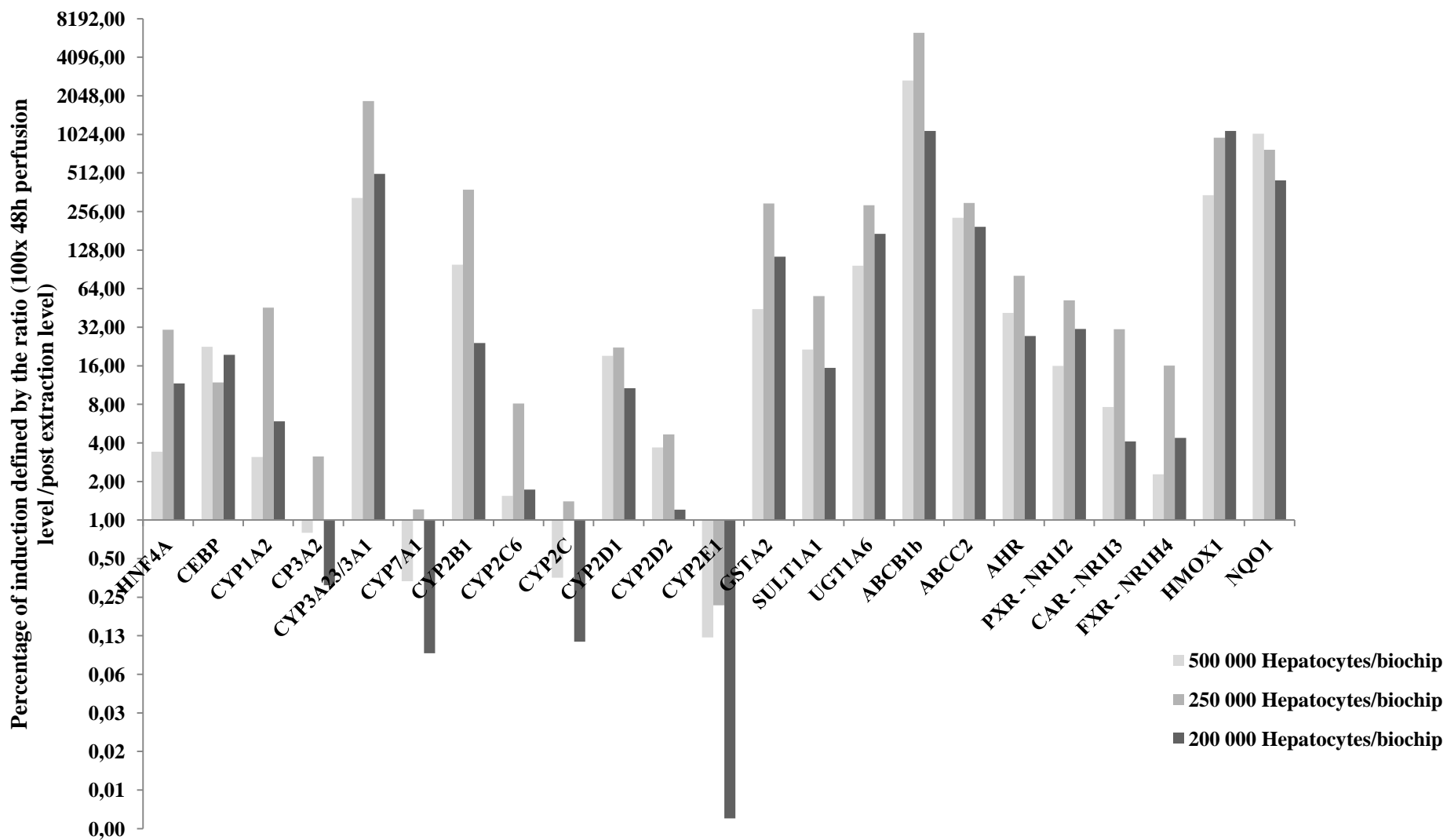


Figure 10: Comparison of the levels of mRNA of rat hepatocytes in the biochips after 48h of perfusion at 25 μ L/min for three inoculated densities. Data expressed the percentage of induction when compared to post extraction values